High order CG schemes for KdV and Saint-Venant flows

Julie Llobell, Sebastian Minjeaud, Richard Pasquetti

Abstract Strategies we have recently proposed to efficiently address dispersive equations and hyperbolic systems with high order continuous Galerkin schemes are first recalled. Using the Spectral Element Method (SEM), we especially consider the Korteweg-De Vries equation to explain how to handle the third order derivative term with an only C^0-continuous approximation. Moreover, we focus on the preservation of two invariants, namely the mass and momentum invariants. With a stabilized SEM, we then address the Saint-Venant system to show how a strongly non linear viscous stabilization, namely the entropy viscosity method (EVM), can allow to support the presence of dry-wet transitions and shocks. The new contribution of the paper is a sensitivity study to the EVM parameters, for a shallow water problem involving many interactions and shocks. A comparison with a computation carried out with a second order Finite Volume scheme that implements a shock capturing technique is also presented.

1 Introduction

The Spectral Element Method (SEM) allows a high order approximation of partial differential equations (PDEs) and combines the advantages of spectral methods, that is accuracy and rapid convergence, with those of the finite element method (FEM), that is geometrical flexibility. The SEM has proved for a long time to be efficient for the highly accurate resolution of elliptic or parabolic problems, but hyperbolic problems and dispersive equations still remain challenging. As relevant examples of such problems, here we consider the Korteweg-De Vries (KdV) and the shallow water equations, and develop some strategies to address them.

R. Pasquetti, S. Minjeaud, J. Llobell
Université Côte d'Azur, CNRS, INRIA, Lab. J.A. Dieudonné, Parc Valrose, 06000 Nice, France,
e-mail: richard.pasquetti / sebastian.minjeaud / julie.llobell@unice.fr

The SEM is based on a nodal Continuous Galerkin (CG) approach, such that the approximation space contains all C^0 functions whose restriction in each element is associated to a polynomial of degree N. More precisely, in the master element $(-1,1)^d$, with d for the space dimension, the basis functions are Lagrange polynomials associated to the $(N+1)^d$ Gauss-Lobatto-Legendre (GLL) points, which are also used as quadrature points to evaluate the integrals obtained when using a weak form of the problem. The fact that interpolation and quadrature points coincide implies that the mass matrix is diagonal. The SEM algorithms that we describe hereafter make strongly use of this property both (i) to address evolution problems with explicit (or implicit-explicit) time schemes and (ii) to define high order differentiation operators in the frame of C^0-continuous approximations.

We describe in Sect. 2 the algorithms that we have developed for the KdV equation, which is a well known example of dispersive equation. In Sect. 3 we consider an hyperbolic system of PDEs, namely the Saint-Venant system, using for stabilization the Entropy Viscosity Method (EVM). In Sect. 4 we address an academic but complex Saint-Venant problem to carry out a sensitivity study to the EVM control parameters. A comparison with results obtained using a Finite Volume (FV) scheme with shock capturing strategy is presented in Section 5, and we conclude in Section 6.

2 SEM approximation of the KdV equation

Here we summarize the SEM method that we have developed for the KdV equation. Details and references may be found in [7].

The KdV problem writes: Find $u(x,t)$, $x \in \Omega$ and $t \in \mathbb{R}^+$, such that

$$\partial_t u + u\partial_x u + \beta \partial_{xxx} u = 0 \tag{1}$$

with the initial condition $u(x,t=0) = u_0(x)$ and, e.g., periodic boundary conditions (β given parameter). With KdV equation, the main difficulties are (i) the approximation of the dispersive term $\beta \partial_{xxx} u$ and (ii) the preservation of at least two invariants: mass and energy

$$I_1 = \int_\Omega u\,dx\,, \quad I_2 = \int_\Omega u^2\,dx\,, \tag{2}$$

which is required to get correct results for long time computations. Due to the presence of the third order derivative term, the standard FEM approximation does not apply. Indeed, after integration by parts a second order derivative remains on the unknown function u or on the test function, say w. To overcome such a difficulty, one generally makes use of a C^1-continuous FEM or a Petrov-Galerkin approach with C^1 test functions. Such approaches generally yield less efficient algorithms, due to the increase of the bandwidth of the resulting algebraic systems, and are often not easy to implement, especially in the multidimensional case or when non trivial boundary conditions are involved. Moreover, the C^1-continuity is not sufficient for PDEs involving higher order derivative terms, since e.g. the C^3-continuity would be required for a fifth order derivative term.

Alternatively, one can introduce new variables. Thus, in the frame of C^0-continuous FEM it is natural to set $f = \partial_{xx} u$, this is the so-called "natural approach" mentioned hereafter. Then, if the convection term is treated explicitly, in such a way it can be assimilated at each time-step to a source term, one obtains the semi-discrete problem:

$$\begin{aligned} M\partial_t \boldsymbol{u} + \beta D\boldsymbol{f} &= \boldsymbol{S} \\ M\boldsymbol{f} + B\boldsymbol{u} &= 0 \end{aligned}$$

with M: mass matrix, B: stiffness matrix and D: Differentiation matrix, and where the vectors of the grid-point values are denoted in bold. By elimination of $\boldsymbol{f}$ one obtains:

$$M\partial_t \boldsymbol{u} - \beta D M^{-1} B\boldsymbol{u} = \boldsymbol{S}\,. \tag{3}$$

At this point the problem is that an inversion of the mass matrix is required. Such an inversion is however trivial if using the SEM, because matrix M is diagonal. Moreover, the $DM^{-1}B$ algebraic operator is sparse.

In the spirit of Discontinuous Galerkin (DG) methods, one can also use the following strategy: Set $g = \partial_x u$ and $f = \partial_x g$, then a C^0-continuous FEM approximation yields:

$$\begin{aligned} M\partial_t \boldsymbol{u} + \beta D\boldsymbol{f} &= \boldsymbol{S} \\ M\boldsymbol{f} &= D\boldsymbol{g} \\ M\boldsymbol{g} &= D\boldsymbol{u}\,. \end{aligned}$$

By elimination of $\boldsymbol{f}$ and $\boldsymbol{g}$ one obtains:

$$M\partial_t \boldsymbol{u} + \beta D(M^{-1}D)^2\boldsymbol{u} = \boldsymbol{S}\,. \tag{4}$$

If using the SEM this new differentiation operator can be easily set up. Its bandwidth is larger than for the previous natural approach, but one can check that its spectral properties are similar.

Using the natural approach or the DG like one, the present definitions of the high order differentiation operator are of course not restricted to 1D problems. When using quadrangular or parrallelipipedic elements, the SEM mass matrices are also diagonal, since the master element is defined by tensorial product. Moreover, a diagonal mass matrix can also be obtained with triangular elements, if using cubature points of the triangle for both the interpolation and quadrature points, see e.g. [10] and references herein.

In time, we suggest using high order implicit-explicit (IMEX) Runge-Kutta (RK) schemes. Then, for stability reasons the dispersive term is handled implicitly whereas the non linear convective term is handled explicitly, under the usual Courant-Friedrich-Lewy (CFL) condition.

Concerning the non linear term, $\int u \partial_x u w \, dx$, where w is the test function, it is of interest to exactly compute it by using the GLL quadrature rule associated to polynomials of degree M such that $2M-1 = 3N-1$, i.e. $M = 3N/2$. Indeed, our numerical experiments have shown that this allows to get satisfactory results without introducing any stabilization term, see [7]. This is interesting since the stabilizing effect results from an improvement in the computation of the convective term and not from the introduction of an artificial dissipation term. The same stabilizing effect is observed in other contexts, see *e. g.* [6, 8] where the use of $M = N+1$ or $M = N+2$ allows to avoid the spurious oscillations.

As mentioned previously, for KdV equation the preservation of at least two invariants is important. Indeed, from a physical point of view it gives sense to the numerical solution since it ensures mass conservation and energy conservation, and from a mathematical point of view it ensures in some sense the stability of the method since here the L^2 norm of the discrete solution is preserved. As a direct consequence of the weak formulation together with the accuracy of the GLL quadrature rule, preserving the mass invariant is natural in the frame of the SEM. Concerning the energy invariant two approaches have been investigated. First, one can take into account the two invariants as constraints and introduce Lagrange multipliers. Second, one can make use of two IMEX schemes, yielding two slightly different solutions, say at time t_n, u_1^n and u_2^n, and write u^n as a linear combination of them: $u^n = (1-\lambda)u_1^n + \lambda u_2^n$. The mass invariant is then preserved and one must look for λ such that $I_2 = Constant$, see (2). It turns out that λ solves

$$S[(u_2-u_1)^2]\lambda^2 + 2S[u_1(u_2-u_1)]\lambda + S[u_1^2] - I_2 = 0$$

where $S[.]$ stands for a quadrature formula on the grid-points.

The computational price of such an approach is a priory twice greater, since it is needed to compute u_1^n and u_2^n to get u^n, but this is not true if using embedded IMEX schemes, that only differ by the final recombination of the intermediate values. The second IMEX scheme (giving u_2^n) is then generally only first order accurate, but one can demonstrate that the accuracy of the leading RK scheme (giving u_1^n) is generally preserved. All details are given in [7].

To conclude this Section we consider the KdV equation with $\beta = 0.022^2$ in the periodic domain $(0,2)$ and assume the initial condition $u_0(x) = \cos(\pi x)$, see e.g. [3, 13]. The numerical solution is computed with $K = 160$ elements, a polynomial approximation degree $N = 5$ and a time step $\tau = 2.5\ 10^{-4}$. The contour levels of the numerical solution in the (x,t)-plane are plotted in Fig. 1 between times 0 and t_R at left, and between times $19t_R$ and $20t_R$ at right, where $t_R \approx 9.68$ is the so called recurrence time, at which one expects to (approximately) recover the initial condition.

Additional test-cases, that e.g. show accuracy results in both periodic and non periodic domains, are provided in [7].

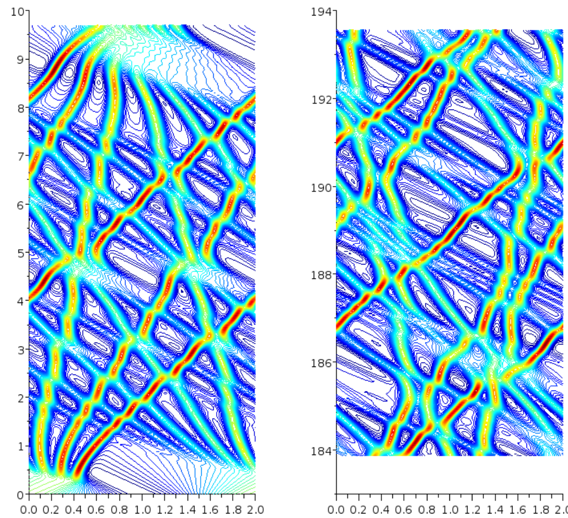

Fig. 1 Contour levels of the numerical solution in the (x,t)-plane, between times 0 and $t_{\rm R}$ at left, between times $19t_{\rm R}$ and $20t_{\rm R}$ at right.

3 EVM-stabilized SEM of the Saint-Venant system

We consider now a more involved fluid flow model that also constitutes a challenging problem for high order CG approaches, namely the shallow water equations. For the paper to be self contained, we give here some details of our EVM-stabilized approximation of the Saint-Venant system, see [9, 11] for details, references and examples of applications.

The Saint-Venant system results from an approximation of the incompressible Euler equations which assumes that the pressure is hydrostatic and that the perturbations of the free surface are small compared to the water height. Then, from the mass and momentum conservation laws and with $\Omega \subset \mathbb{R}^2$ for the computational domain, one obtains equations that describe the evolution of the height $h : \Omega \to \mathbb{R}^+$ and of the horizontal velocity $\boldsymbol{u} : \Omega \to \mathbb{R}^2$: For $(\boldsymbol{x},t) \in \Omega \times \mathbb{R}^+$:

$$\begin{aligned} &\partial_t h + \nabla \cdot (h\boldsymbol{u}) = 0 \\ &\partial_t (h\boldsymbol{u}) + \nabla \cdot (h\boldsymbol{u} \otimes \boldsymbol{u} + gh^2 \mathbb{I}/2) + gh\nabla z = 0 \end{aligned} \tag{5}$$

with $\mathbb{I}$, identity tensor, g, gravity acceleration, and where $z(\boldsymbol{x})$ describes the topography, assumed such that $\nabla z \ll 1$. Moreover, for the saint-Venant system there exists a convex entropy (actually the energy E) such that

$$\partial_t E + \nabla \cdot ((E + gh^2/2)\boldsymbol{u}) \leq 0, \quad E = h\boldsymbol{u}^2/2 + gh^2/2 + ghz. \tag{6}$$

so that one may think to implement the EVM for stabilization of the following SEM discrete approximation.

Set $\boldsymbol{q} = h\boldsymbol{u}$ and let $h_N(t)$ (resp. $\boldsymbol{q}_N(t)$) to be the piecewise polynomial continuous approximation of degree N of $h(t)$ (resp. $\boldsymbol{q}(t)$). The proposed stabilized SEM relies on the Galerkin approximation of the Saint-Venant system completed with viscous terms for both the mass and momentum equations. For any $w_N, \boldsymbol{w}_N$ (scalar and vector valued functions, respectively) spanning the same approximation spaces, in semi-discrete form:

$$\begin{aligned} &(\partial_t h_N + \nabla \cdot \boldsymbol{q}_N, w_N)_N = -(\nu_h \nabla h_N, \nabla w_N)_N \\ &(\partial_t \boldsymbol{q}_N + \nabla \cdot I_N(\boldsymbol{q}_N \otimes \boldsymbol{q}_N / h_N) + gh_N \nabla (h_N + z_N), \boldsymbol{w}_N)_N = -(\nu_q \nabla \boldsymbol{q}_N, \nabla \boldsymbol{w}_N)_N \end{aligned} \tag{7}$$

where $\nu_h \propto \nu_q = \nu$, with ν : entropy viscosity (in the rest of the paper we simply use $\nu_h = \nu_q$). The usual SEM approach is used here: I_N is the piecewise polynomial interpolation operator, based for each element on the tensorial product of Gauss-Lobatto-Legendre (GLL) points, and $(.,.)_N$ stands for the SEM approximation of the $L^2(\Omega)$ inner product, using for each element the GLL quadrature formula which is exact for polynomials of degree less than $2N-1$ in each variable. Note that thanks to using $\nabla \cdot I_N(gh_N^2 \mathbb{I}/2) \approx gh_N \nabla h_N$ (while h_N^2 is generally piecewise polynomial of degree greater than N), and thus grouping in (7) the pressure and topography terms, a well balanced scheme is obtained by construction: If $\boldsymbol{q}_N \equiv 0$ and $h_N \neq 0$, then $h_N + z_N = Constant$. Of course, a difficulty comes from the required positivity of h_N, as discussed at the end of the present Section.

It remains to define the entropy viscosity ν. To this end we make use of an entropy that does not depend on z but on ∇z, which is of interest, at the discrete level, to get free of the choice of the coordinate system. Taking into account the mass conservation equation (into the entropy equation) one obtains:

$$\partial_t \tilde{E} + \nabla \cdot ((\tilde{E} + gh^2/2)\boldsymbol{u}) + gh\boldsymbol{u} \cdot \nabla z \leq 0\,, \quad \tilde{E} = h\boldsymbol{u}^2/2 + gh^2/2\,. \tag{8}$$

At each time-step, we then compute the entropy viscosity $\nu(\boldsymbol{x})$ at the GLL grid points, using the following three steps procedure:

- Assuming all variables given at time t_n, compute the entropy residual, using a Backward Difference Formula, e.g. the BDF2 scheme, to approximate $\partial_t \tilde{E}_N$

  $$r_E = \partial_t \tilde{E}_N + \nabla \cdot I_N((\tilde{E}_N + gh_N^2/2)\boldsymbol{q}_N/h_N) + g\boldsymbol{q}_N \cdot \nabla z_N$$

  where $\tilde{E}_N = \boldsymbol{q}_N^2/(2h_N) + gh_N^2/2$. Then set up a viscosity ν_E such that:

  $$\nu_E = \beta |r_E| \delta x^2 / \Delta E\,,$$

  where ΔE is a reference entropy, β a user defined control parameter and δx the local GLL grid-size, defined such that δx^2 equals the surface of the quadrilateral cell (of the dual GLL mesh) surrounding the GLL point, and using symmetry assumptions for the points at the edges and vertices of the element.

- Define a viscosity upper bound based on the wave speeds : $\lambda_{\pm} = u \pm \sqrt{gh}$:

$$\nu_{max} = \alpha \max_{\Omega}(|\boldsymbol{q}_N/h_N| + \sqrt{gh_N})\delta x$$

where α is a $O(1)$ user defined parameter (recall that for the advection equation $\alpha = 1/2$ is well suited).

- Compute the entropy viscosity:

$$\nu = \min(\nu_{max}, \nu_E)$$

and smooth: (i) locally (in each element), e.g. in 1D: $(\nu_{i-1} + 2\nu_i + \nu_{i+1})/4 \to \nu_i$; (ii) globally, by projection onto the space of the C^0 piecewise polynomials of degree N. Note that operation (ii) is cheap because the SEM mass matrix is diagonal.

The positivity of h_N is difficult to enforce as soon as $N > 1$, so that for problems involving dry-wet transitions the present EVM methodology must be completed. The algorithm that we propose is the following: In dry zones, i.e. for any element Q_{dry} such that at one GLL point $\min h_N < h_{thresh}$, where h_{thresh} is a user defined threshold value (typically a thousandth of the reference height):

- Modify the entropy viscosity technique, by using in Q_{dry} the upper bound first order viscosity:

$$\nu = \nu_{max} \quad \text{in} \quad Q_{dry}$$

- In the momentum equation assume that:

$$h_N g \nabla(h_N + z_N) \equiv 0 \quad \text{in} \quad Q_{dry}$$

- Moreover, notice that the upper bound viscosity $\nu_{\max}$ is not local but global, and that the entropy scaling ΔE used in the definition of ν_E is time independent. This has improved the robustness of the general approach described in [5].

Simulations with dry-wet transitions and comparisons to exact solutions are given in [9] and [11], for 1D and 2D flows, respectively.

4 Sensitivity study to the EVM control parameters

We address a shallow water problem, the "falling columns" test proposed in [1], whose solution is characterized by many interactions and shocks. Thus, it constitutes a good benchmark to check the sensitivity of our SEM model to the control parameters of the EVM. The flow is governed by the Saint-Venant system (5), in which the dimensionless gravity acceleration is taken equal to 2. The computational domain is the square $(-1,1)^2$, with free slip condition at the boundary. At the initial time the fluid is at rest, $\boldsymbol{u}(t=0)=0$, and the height is given by:

$$h(t=0) = 3 + 1_{(\boldsymbol{x}-\boldsymbol{x}_1)^2<0.15^2} + 1_{(\boldsymbol{x}-\boldsymbol{x}_2)^2<0.15^2} + 2\,1_{\boldsymbol{x}^2<0.2^2}$$

with $\boldsymbol{x}_1=(0.5,0.5)$ and $\boldsymbol{x}_2=(-0.5,-0.5)$, and where 1_ω is the indicator function of subdomain ω.

A first computation has been carried out without the EVM stabilization. As expected, in this case the computation crashes, since a stabilization is needed when shocks develop. Computations have been done for the following values of the pair (α,β): (0.5, ∞), (1, ∞), (0.5, 1), (0.5, 2), (0.5, 3), (1, 3) and (1,5). Mentioning $\beta=\infty$ means that we simply use a first order viscosity everywhere. Note that choosing $\alpha=0.5$ is very natural, since for an advection equation it yields a $O(h)$ diffusion term equivalent to the implicit one of the upwind scheme. The three pairs such that $1\leq\beta\leq3$ show the influence of β, while keeping $\alpha=0.5$. In the two last tests the stabilization is strengthened, by increasing α up to 1 and β up to 5.

One uses a polynomial approximation of degree $N=5$ in each quadrangle of a regular $K=100\times100$ mesh. This yields 255001 interpolation points in Ω, with 91001 of them at the quadrangle boundaries. All computations have been made with a time step $\tau=10^{-4}$. Such time and space discretizations allow a fair comparison with FV results in Section 5.

The height of the flow at the final time, $t_f=1.035$, is visualized for the different simulations in Fig. 2. As desired, the result obtained without EVM but only a first order viscosity is very smooth, but clearly completely false. If implementing the EVM, then the correct solution is captured. One observes that strengthening the stabilization allows to filter some spurious oscillations. Note that the presence of such oscillations is not surprising, since the discontinuities of the initial height enforces the Gibbs phenomenon. The present study of the influence of the EVM control parameters is of course very qualitative, and moreover only based of the height at the final time.

In order to complete such a qualitative study, we show in Fig. 3 the evolutions of the extrema of the height during the simulation. Clearly, (i) the first order viscosity result is not correct and (ii) the stronger is the EVM-stabilization, the smoother are the extrema evolutions. Additionally, one observes the EVM-stabilization becomes too strong for $(\alpha=1,\beta=5)$, since the corresponding curve no longer coincides with the other EVM ones.

5 Comparison with a second order FV computation

For comparison purposes, we provide in this section the results obtained using a first order and a second order FV scheme, that can be viewed as an extension to the 2D and to the 2nd order accuracy of the scheme presented in [2]. These schemes work on staggered Cartesian grids and, in contrast to the colocalized approach for conser-

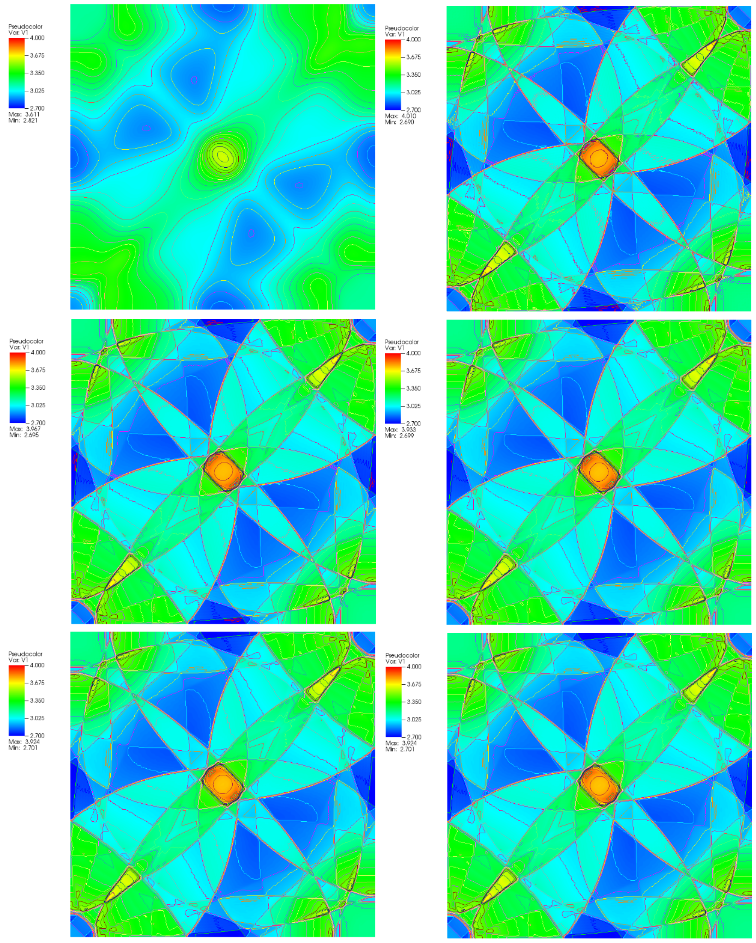

Fig. 2 Visualizations of the height at the final time $t_f = 1.035$ for the (α, β) pairs (0.5, ∞), (0.5, 1), (0.5, 2) , (0.5, 3), (1, 3) and (1, 5), from up to down and left to right. For all graphics the color bar is the same and the extrema are mentioned.

vative system, it make use of a discretization of the physical variables, the height and the velocity separately, instead of a discretization of the conservative variables. The height is stored at the cell centers whereas the horizontal (resp. vertical) component of the velocity is stored at the vertical (resp. horizontal) edges like in the well-known MAC (Marker-and-Cell) scheme. The numerical fluxes are derived using the framework of the so-called (kinetic) Boltzmann schemes. In the spirit of hydrodynamic limits which allow to derive the Euler equations from Boltzmann equation, the Saint Venant system is seen as the limit of a vector BGK (Bhatnagar-Gross-Krook) equation, see e.g. [12]. This is a transport equation for a kinetic variable f (i.e. a variable which depends on $(\boldsymbol{x}, t)$ but also on an auxiliary "ghost" velocity variable ξ) with a

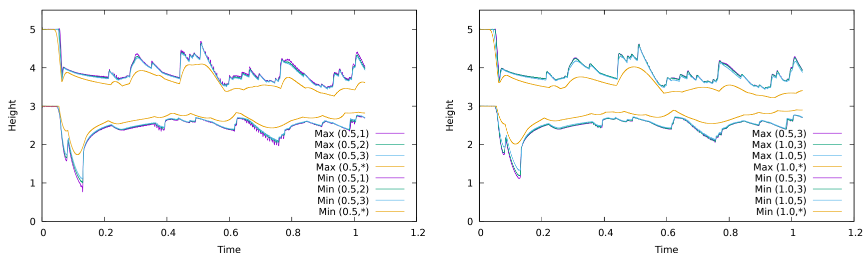

Fig. 3 Evolution of the maximum and minimum of the height when using the first order ($\beta = *$) and the EVM stabilization for different (α, β) pairs. The influence of β is mainly shown in the left panel and the influence of α in the right one.

relaxation term towards a given equilibrium state which depends only on ξ and on the zeroth moment of f. This equilibrium state is especially designed to ensure that, at least formally, the zeroth moment of f satisfies the Saint-Venant equation when the relaxation parameter goes to zero. A numerical scheme for the BGK equation is obtained by decoupling into two successive steps the transport and the relaxation process. A basic upwind scheme is then used for the (linear) transport step. Finally, we get rid of the “ghost” velocity variable by integrating the formula with respect to ξ: it provides formula of fluxes for updating the height and the momentum (see [2]). Note that this formula, which may be written explicitly, can be viewed as an upwinding of the transported variables (height and momentum) with respect to the sign of the characteristic velocities, the pressure being centered. The second order accuracy is reached thanks to a MUSCL-like (Monotonic Upwind Scheme for Conservation Laws) procedure using the MinMod limiter. The first order FV scheme is coupled with an explicit Euler time discretization whereas a second order ERK (explicit Runge-Kutta) scheme is used with the second order space discretization. All the details can be found in [4].

The results obtained for the height at the final time $t_f = 1.035$ are presented in Fig. 4. The grid is a 512×512 Cartesian mesh and the time step is $\tau = 10^{-4}$, so that the number of degrees of freedom for the height is 262144 allowing a fair comparison with the results obtained using the SEM in Fig. 2. As expected, the result obtained with the first order FV scheme is smooth and close to the one obtained with the SEM when adding a first order viscosity whereas using the second FV scheme allows to recover the correct solution (free of spurious oscillations) very close to the one obtained with the EVM.

6 Conclusion

A lot of numerical methods have been developed in the past, and are still developed, to address the KdV and Saint-Venant problems. In this spirit, but in contrast with

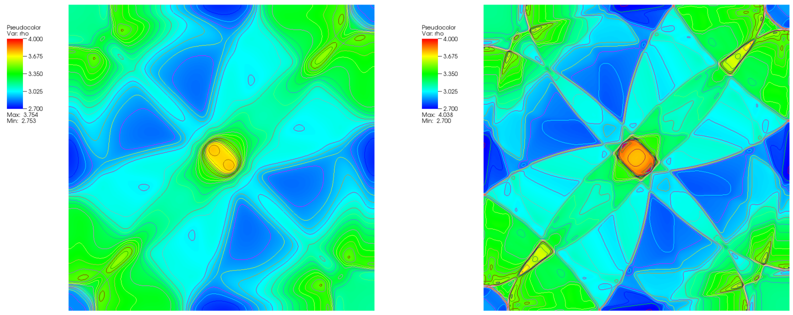

Fig. 4 Visualizations of the height at the final time $t_f = 1.035$ using a first order FV scheme (at left) and a second order FV scheme (at right). The color bar is the same as in Fig. 2.

studies based on the celebrated FV or DG methods, here we have proposed to use a high order CG method, namely the SEM. For KdV the main advantage of the SEM is the diagonal structure of the mass matrix. This indeed allows to simply eliminate intermediate variables and thus set up efficient algorithms. For hyperbolic problems a stabilization technique is however required. For Saint-Venant flows, we have investigated the EVM capabilities and additionally provided a sensitivity study to the EVM parameters as well as a comparison with FV results. Additional tests and comparisons for less academical problems will be focused on in our future works.

References

1. N. Aguillon, Problèmes d'interfaces et couplages singuliers dans les systèmes hyperboliques : analyse et analyse numérique, PhD thesis, Univ. Paris Sud, 2014.
2. F. Berthelin, T. Goudon, S. Minjeaud, Kinetic schemes on staggered grids for barotropic Euler models: entropy-stability analysis, *Math. Comput.* 84, 2221–2262, 2015.
3. Y. Cui and D.K. Mao, Numerical method satisfying the first two conservation laws for the Korteweg-de Vries equation. *J. Comput. Phys.* 227 (1), 376-399, 2007.
4. J. Llobell, Schémas Volumes Finis à mailles décalées pour la dynamique des gaz, PhD thesis, Université Côte d'Azur, 2018.
5. J.L. Guermond, R. Pasquetti, B. Popov, Entropy viscosity method for non-linear conservation laws, *J. of Comput. Phys.* 230 (11), 4248-4267, 2011.
6. R.M. Kirby, G.E. Karniadakis, De-aliasing on non uniform grids: algorithms and applications, *J. Comput. Phys.* 191 (2003) 249-264.
7. S. Minjeaud and R. Pasquetti, High order C^0-continuous Galerkin schemes for high order PDEs, conservation of quadratic invariants and application to the Korteweg-De Vries model, *J. of Sci. Comput.* 74, 491-518, 2018.
8. J.P. Ohlsson, P. Schlatter, P.F. Fischer, D.S. Henningson, Stabilization of the spectral element method in turbulent flow simulations, in *Lecture Notes in Computational Science and Engineering* 76, Springer-Verlag Berlin Heidelberg 2011, 449-458.
9. R. Pasquetti, J.L. Guermond, B. Popov, Stabilized spectral element approximation of the Saint-Venant system using the entropy viscosity technique, in *Lecture Notes in computational Science and Engineering : Spectral and High Order Methods for Partial Differential Equations - ICOSAHOM 2014*, vol. 106, Springer, 397-404, 2015.
10. R. Pasquetti and F. Rapetti, Cubature versus Fekete-Gauss nodes for spectral element methods on simplicial meshes, *J. of Comput. Phys.* 347, 463-466, 2017.

11. R. Pasquetti, Viscous stabilizations for high order approximations of Saint-Venant and Boussinesq flows, in *Lecture Notes in computational Science and Engineering : Spectral and High Order Methods for Partial Differential Equations - ICOSAHOM 2016*, vol. 119, Springer, 519-531, 2017.
12. L. Saint Raymond, Hydrodynamic limits of the Boltzmann equation, *Lect. Notes in Math.* 1971, Springer, 2009.
13. N.J. Zabusky and M.D. Kruskal, Interaction of solitons in a collisionless plasma and the recurence of initial states. *Phys. Rev. Lett.* 15 (6), 240243, 1965.